

Detection of COVID-19 from Chest X-ray and CT Scan Images using Improved Stacked Sparse Autoencoder

Syahril Ramadhan Saufi^{1*}, Muhd Danial Abu Hasan¹, Zair Asrar Ahmad¹, Mohd Salman Leong² and Lim Meng Hee²

¹*School of Mechanical Engineering, Universiti Teknologi Malaysia (UTM), 81310 Skudai, Johor Bahru, Malaysia*

²*Institute of Noise and Vibration, Universiti Teknologi Malaysia (UTM), 54100 Kuala Lumpur, Malaysia*

ABSTRACT

The novel Coronavirus 2019 (COVID-19) has spread rapidly and has become a pandemic around the world. So far, about 44 million cases have been registered, causing more than one million deaths worldwide. COVID-19 has had a devastating impact on every nation, particularly the economic sector. To identify the infected human being and prevent the virus from spreading further, easy, and precise screening is required. COVID-19 can be potentially detected by using Chest X-ray and computed tomography (CT) images, as these images contain essential information of lung infection. This radiology image is usually examined by the expert to detect the presence of COVID-19 symptom. In this study, the improved stacked sparse autoencoder is used to examine the radiology images. According to the result, the proposed deep learning model was able to achieve a classification accuracy of 96.6% and 83.0% for chest X-ray and chest CT-scan images, respectively.

ARTICLE INFO

Article history:

Received: 4 December 2020

Accepted: 1 April 2021

Published: 19 July 2021

Keywords: COVID-19, CT scan, deep learning, image classification, X-ray

DOI: <https://doi.org/10.47836/pjst.29.3.14>

E-mail addresses:

msramadhan93@gmail.com (Syahril Ramadhan Saufi)

muhd_danial200@yahoo.com (Muhd Danial Abu Hasan)

zair@utm.my (Zair Asrar Ahmad)

salman.leong@gmail.com (Mohd Salman Leong)

limmenghee@gmail.com (Lim Meng Hee)

*Corresponding author

INTRODUCTION

Coronavirus (COVID-19) is a disease caused by a severe acute respiratory syndrome (SARS-CoV-2). This virus was detected in December 2019 in Wuhan, Hubei Province, China. According to Huang et al. the most

common symptoms on the infected patient in Wuhan, China were fever, cough and myalgia or fatigue (Huang et al., 2020). COVID-19 has spread worldwide, and it has caused a dead around three million peoples around the world. However, the vaccination programme has been conducted worldwide to prevent the spread of COVID-19. Four possible methods can be used to detect the COVID-19 virus from human such as enzyme-linked immunosorbent assay (ELISA), loop-mediated isothermal amplification (LAMP), lateral flow and reverse transcription-polymerase chain reaction (RT-PCR). RT-PCR is the common method used in COVID-19 detection on the human body. However, this method requires 45 to 90 minutes to obtain the result (Bustin & Nolan, 2020) and it has a lack of accuracy on the early-stage infected patient (Zu et al., 2020). Due to large volume of samples, the analysis of RT-PCR can take several days.

According to Zu et al. (2020), radiologic examination can be used in detecting infected patient. Besides, Salehi et al. (2020) did review that there is an abnormal occur on infected patient' chest which can be seen using computer tomography (CT) image. The diagnosis using CT scan on infected patient's chest outperformed RT-PCR method in many cases (Salehi et al., 2020). According to X. Yang et al. (2020), the early disease can be detected using CT scan method and the authors have conducted a comprehensive review on chest radiography analysis. Also, several studies have shown the capability of COVID-19 detection using chest X-ray images (Luo et al., 2019; Purohit et al., 2020; Apostolopoulos & Mpesiana, 2020). However, both CT-scan and X-ray images require an expert to examine the image.

Machine learning is a method that has become a popular choice in providing an automated diagnosis for any disease. The machine learning can provide a more accurate and consistent result. The implementation of the machine learning model can assist the radiologist in making a correct decision since there is a lot of patient out there waiting for the result. With a massive number of tests, it may cause a high tendency of making a wrong examination from the image due to limited diagnosis time. The architecture of simple machine learning has recently been explored to create a deeper machine learning model architecture that can produce a complete model without requiring any manual feature preparation (Ozturk et al., 2020; Saufi et al., 2019). By taking advantage of the deep learning model, this study implements the deep learning method in diagnosing the non-infected and infected patient of COVID-19 virus using the radiology image such as CT scan and X-ray images. The deep learning model has a high capability of producing a result with a split second when the model is properly trained. Hence, the effective quantitative analysis of these images can be used as a complementary result before getting the result from RT-PCR. To date, RT-PCR has a best standard on the examination of COVID-19 as it directly analysing the virus at DNA level.

The stacked sparse autoencoder (SSAE) model has been used in this analysis. SSAE model is among the popular model in deep learning. However, the SSAE model comes with several challenges such as hyperparameter tuning and computer processing time. The hyperparameter should be tuned properly to obtain an accurate diagnosis result. This hyperparameter is usually tuned manually which is time-consuming. Hence, this study utilised the differential evolution method to optimise the hyperparameter of SSAE model. The proposed model is developed to deal with several types of data such as a statistical parameter, images, and raw series data. Also, it has the ability in dealing with low sample dataset and it did not require any image enhancement on the dataset for image classification analysis.

MATERIALS AND METHODS

Stacked Sparse Autoencoder Architecture

The stacked sparse autoencoder is built by stacking the sparse autoencoder with many numbers. As shown in Figure 1, the Sparse autoencoder comprises the encoder, hidden layer, and decoder features. The encoder mapped the input data using $h = f(w_1x + b)$ into hidden representation ($h \in R^k$) and the following function $\hat{x} = g(w_2h + b)$ is used to reconstruct the hidden representation. Sparse autoencoder (SAE) imposes a restriction on the hidden autoencoder units that cause inactive hidden unit activation (Wang et al., 2018). The reconstruction error of sparse autoencoder is shown in Equation 1.

$$E(w, b) = \frac{1}{2} \|h_{w,b}(x) - y\|^2 + \beta \sum_{j=1}^n KL(\rho \|\hat{\rho}_j) + \frac{\lambda}{2} \sum_{l=1}^{nl} \sum_i^{sl-1} \sum_j^{sl} (W_{ij}^{(l)})^2 \tag{1}$$

where the Kullberg-Leibler divergence is represented as $KL(\rho \|\hat{\rho}_j) = \rho \log \frac{\rho}{\hat{\rho}_j} + (1 - \rho) \log \frac{1-\rho}{1-\hat{\rho}_j}$, β is a sparsity penalty term weight, ρ is the sparsity parameter and $\hat{\rho}_j$ is the average activation of the hidden unit. The sparse autoencoder cannot identify the useful data as the purpose of the network for obtaining useful information. By restricting the weight, w and bias, b using the sparsity term, the useful data is obtained at the hidden layer. At the end of the multiple sparse autoencoder layer, another layer called Softmax classifier is stacked. This layer is intended to identify the useful features of information processed by the sparse autoencoder. In Equation 2, the equation of Softmax is defined.

$$h_{\theta}(x^i) = \begin{bmatrix} p(y^i = 1|x^i; \theta) \\ p(y^i = 2|x^i; \theta) \\ \vdots \\ p(y^i = k|x^i; \theta) \end{bmatrix} = \frac{1}{\sum_{i=1}^k e^{\theta_j^T x^i}} \begin{bmatrix} e^{\theta_1^T x^i} \\ e^{\theta_2^T x^i} \\ \vdots \\ e^{\theta_k^T x^i} \end{bmatrix}, \tag{2}$$

where $\theta_1, \theta_2, \dots, \theta_k \in \mathfrak{R}^{n+1}$ are the model parameters and $1 / \sum_{i=1}^k e^{\theta_j^T x^i}$ normalizes the distribution to ensure that the sum value is equal to one.

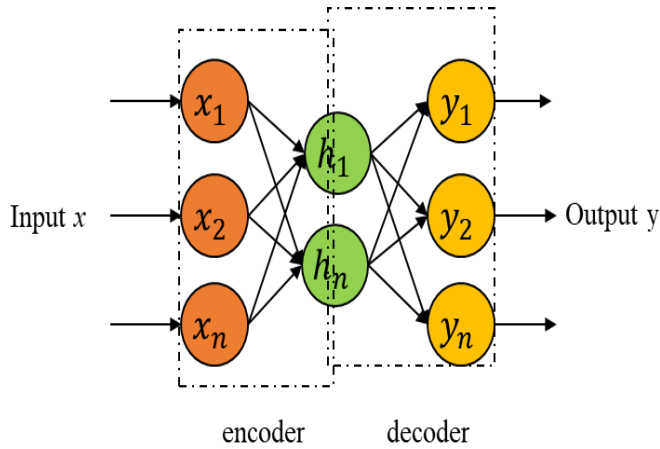


Figure 1. Sparse autoencoder architecture

Proposed Model

Several modifications were involved in the built model. First to decrease the training time of the model, the resilient backpropagation (Rprop) algorithm is implemented. Then using the differential evolution (DE) optimization process, the hyperparameters including weight regulariser, the number of hidden units, sparsity regulariser and sparsity proportion are optimized. DE is among the finest methods of optimization, based on studies examined by Wahab et al. (2015). These techniques have been used to detect rotating machinery failure, and the result has shown that the efficiency of the deep learning model can be enhanced. Throughout the analysis, however some hyperparameters are kept constant, such as the number of epochs, the number of sparse autoencoders, and loss function. The epoch was set to 500, to form the proposed model, two sparse autoencoders were stacked and the msespars was used as the loss function. For each sparse autoencoder, there are four significant hyperparameters and using differential evolution, the hyperparameters value are optimized. Furthermore, using a resilient backpropagation algorithm, the training function of this network was optimized. Figure 2 shows the entire architecture of the proposed model (improved stacked sparse autoencoder). It is important to note that when training and testing using the machinery dataset, the proposed model did not require any image processing. The proposed method is therefore used in this paper to detect the presence of the COVID-19 virus on photographs of chest X-ray and CT scans.

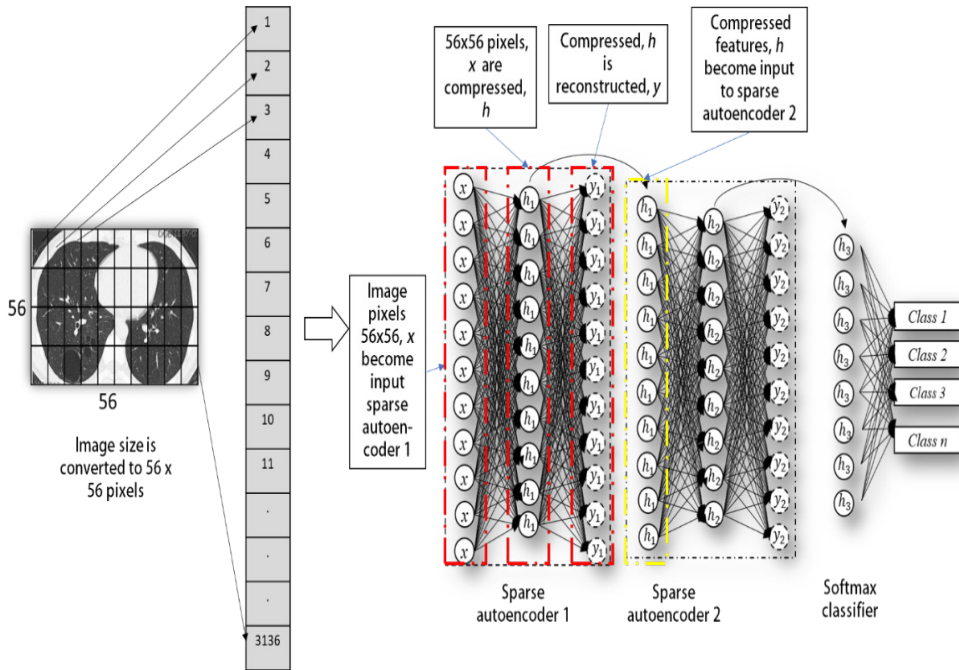


Figure 2. The proposed model architecture

Differential Evolution Optimisation. Differential evolution (DE) is used in to deal with the hyperparameter selection issue discussed in the previous section. DE is a metaheuristic optimization that uses genetic algorithm operations. As the population grows, the algorithm inevitably changes its search behaviour from discovery to exploitation due to its self-referential mutation. The primary aim of DE is to use mutation and crossover to produce new vectors. For the next generation, the selection process decides the vectors that will succeed. For each target vector $X_{i,g}$, a mutant vector is generated via the Equation 3:

$$V_{i,G} = X_{r_1^i,G} + F \cdot (X_{r_2^i,G} - X_{r_3^i,G}), \tag{3}$$

where $i = 1, \dots, NP$, r_1, r_2, r_3 are random numbers, $r_1 \neq r_2 \neq r_3 \neq i$, x is a decision vector, and F is an amplification factor ($[0 \ 1]$) that determines the differential variation of $(X_{r_2^i,G} - X_{r_3^i,G})$.

The parent vector information for the trial vector U is crossover with the mutated vector using Equation 4 and 5.

$$U_{i,G+1} = (U_{1i,G+1}, U_{2i,G+1}, \dots, U_{Di,G+1}), \tag{4}$$

and

$$U_{ji,G} \begin{cases} V_{ji,G+1} & \text{if } (rand_{i,j}[0,1] \leq Cr \text{ or } j = j_{rand}) \\ X_{ji,G} & \text{otherwise} \end{cases}, \quad (5)$$

where $j = \{1, 2, \dots, D\}$, $Cr [0,1]$ is the crossover rate, the random number is $rand_{i,j} [0,1]$, and $j_{rand} (1, 2, \dots, D)$ is randomly selected to ensure that $U_{ji,G}$ gets at least one component from $V_{i,G}$.

For the next generation, selection is the process of choosing a vector between $(U_{i,G+1})$ and $(X_{i,G})$. A vector with a higher fitness value is chosen via Equation 6.

$$X_{i,G+1} = \begin{cases} U_{i,G} & \text{if } f(U_{i,G}) < f(X_{i,G+1}) \\ X_{i,G} & \text{if } f(U_{i,G}) \geq f(X_{i,G+1}) \end{cases} \quad (6)$$

Resilient Backpropagation. The supervised learning algorithm relies heavily on the backpropagation algorithm, as the algorithm can assist the model to find the appropriate parameter value for the lowest training function, such as weight, w and bias, b . There are a lot of algorithms for backpropagation that can be used to adjust the weight and bias so that a stable model is achieved by the model. However, the deep learning model has a deep architecture that causes the training function to be more complicated compared to the shallow learning model and not all the available backpropagation model can tune the deep learning model. Since the SAE model is a deep learning family, it is crucial to select the best backpropagation algorithm. Therefore, in this study, a backpropagation algorithm called the resilient backpropagation algorithm was selected.

Resilient backpropagation was proposed by Riedmiller and Braun (1993). The concept of this method is to repeatedly analyze the chain rule to calculate the effect of weight and bias with respect to an error function in the machine-learning model architecture. Compared to other methods, this method uses separate weight updates. By considering the sign of the error gradient, the algorithm updates the weight of the network and the weight update is defined as Equation 7.

$$\Delta_{ij}(t) = \begin{cases} \eta^+ \Delta_{ij}(t-1), & \text{if } \frac{\delta E}{\delta w_{ij}}(t-1) \cdot \frac{\partial E}{\partial w_{ij}}(t) > 0 \\ \eta^- \Delta_{ij}(t-1), & \text{if } \frac{\delta E}{\delta w_{ij}}(t-1) \cdot \frac{\partial E}{\partial w_{ij}}(t) < 0 \\ \Delta w_{ij}(t-1), & \text{otherwise} \end{cases} \quad (7)$$

When the element of $\partial E / \partial w_{ij}$ maintains its sign from one iteration to the next consecutive iteration, the factor of η^+ helps increase the component Δ_{ij} . Meanwhile, when the partial derivative when the partial derivative $\partial E / \partial w_{ij}$ changes its sign from one iteration to the next consecutive iteration, the factor of η^- helps to minimize the variable Δ_{ij} . The η^+ value is 1.2 while the η^- value is 0.5 are set in this study. The weight will update based on Equation 8.

$$\Delta w_{ij}(t) = \begin{cases} -\Delta_{ij}, & \text{if } \frac{\delta E}{\delta w_{ij}} > 0 \\ +\Delta_{ij}, & \text{if } \frac{\delta E}{\delta w_{ij}} < 0 \\ 0, & \text{otherwise} \end{cases} \quad (8)$$

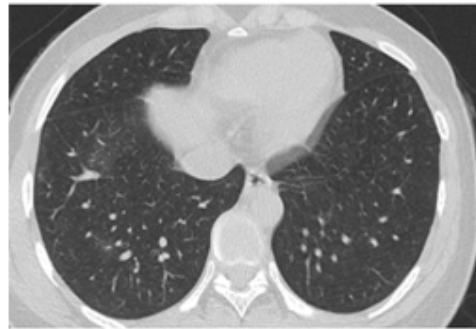
The details of the algorithm can be referred to the owner of this method (Riedmiller & Braun, 1993).

Data Collection and Preparation

The COVID-19 dataset from chest CT-scan and X-ray images were referred from X. Yang et al. (2020) and Ozturk et al. (2020), respectively. The details of the Chest CT and X-ray examination on the data collection, imaging parameters and the imaging system have been thoroughly discussed by W. Yang et al. (2020) and Ozturk et al. (2020). For the analysis of the proposed model, the CT-scan and chest X-ray dataset were obtained from open access sources in which the utility of the dataset was evaluated and confirmed by a senior radiologist. The open-source dataset can be obtained from He et al. (2020) and Cohen et al. (2020). The image example has been shown in Figure 3 and 4. In this study, there is no image enhancement has been done on the image as the original image is directly used to study the performance of the proposed model on the original image. However, there are only a simple image pre-processing has been done by resizing the image into 56x56 pixels. It is important to note that the size of the image affect the deep learning model processing because a large size of an image takes a long training time (Verstraete et al., 2017). Also, the data has been normalised to increase the efficiency of the proposed model and prevent the network from overfitting (Srivastava et al., 2014).



a) Non-COVID-19



b) COVID-19

Figure 3. CT-Scan of chest images

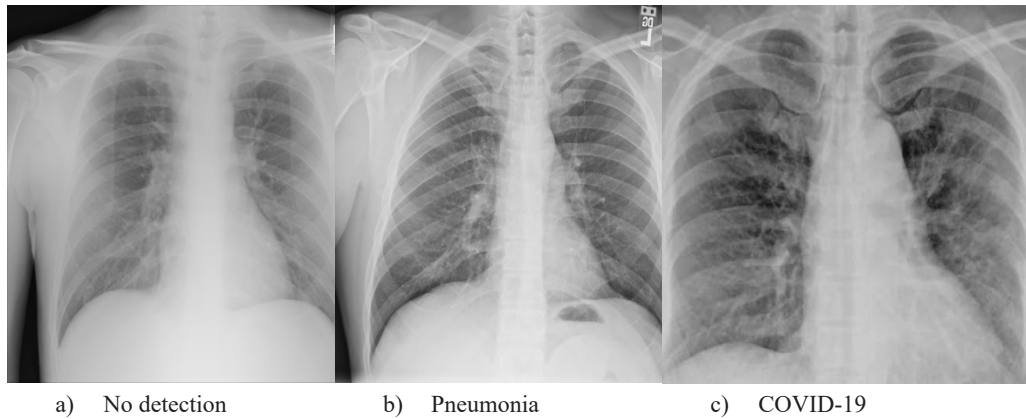


Figure 4. X-ray of chest images

Tables 1 and 2 below show data distribution for CT scan images and X-ray images, respectively. The training data will be used to generalise the sparse autoencoder parameters (weight and bias) that will be optimised using a back-propagation algorithm. The model is validated using the validation data of data to calculate the sparse autoencoder model's accuracy on the selected hyperparameter value. If the model does not achieve acceptable accuracy, the hyperparameter will be changed using the differential evolution algorithm. The process will continue until the model reaches the 0% training accuracy on the validation data. Then, the model will be evaluated using test dataset.

Table 1

Data distribution for CT scan images

Data	No finding	COVID-19
Train	100	100
Valid	50	50
Test	50	50
Total	200	200

Table 2

Data distribution for X-ray images

Data	No finding	Pneumonia	COVID-19
Train	100	100	60
Valid	50	50	25
Test	50	50	40
Total	200	200	125

RESULTS AND DISCUSSION

The performance of the proposed model during the training process has been shown in Figures 5 and 6 on chest CT-Scan and X-ray images, respectively. The proposed model performed well on both datasets as the performance achieved 0% training error means that the model has already generalized the information from the training and validation image. Hence, the model is ready to be evaluated using the test dataset. It can be noticed that the model required different epochs number to reach the lowest training error. Then, the model is tested with test dataset and the result on the CT-scan and X-ray images have been tabulated in Tables 3 and 4, respectively. There are five types of the score are calculated to quantify the performance of the proposed model such as sensitivity, specificity, precision, accuracy, and F1-score. The definition and formula on each score can be referred to in (Tharwat, 2018). From Table 3, it can be noticed that the proposed model achieved around 81% to 86% for all scores. Hence, it shows that there is no bias toward one class on classification performance. The performance of the proposed model is satisfactory as several other research reaches more or less the same as the proposed model performance (Ying et al., 2020; Zheng et al., 2020).

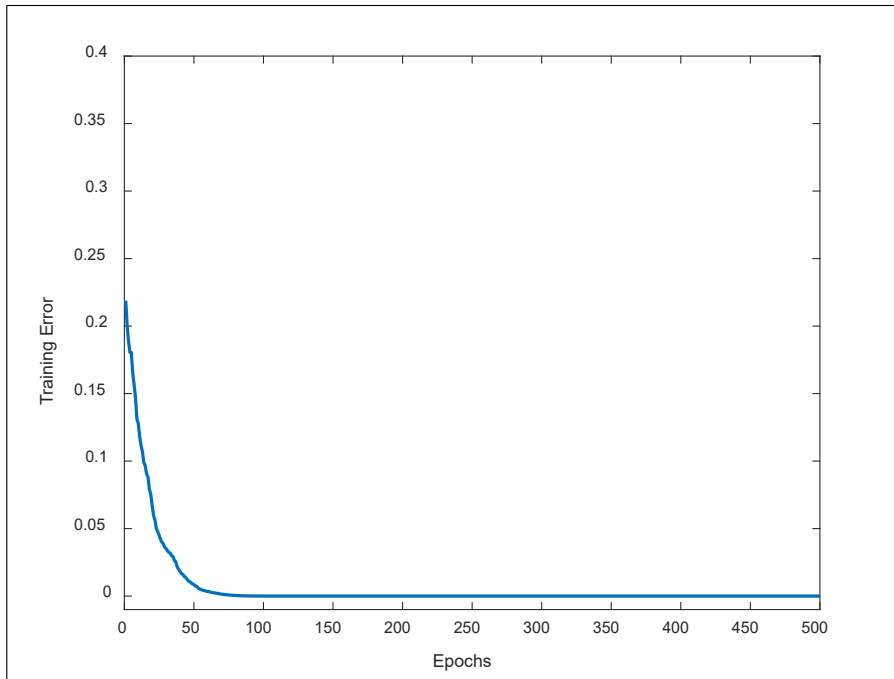


Figure 5. Training performance of the proposed model on CT-Scan images

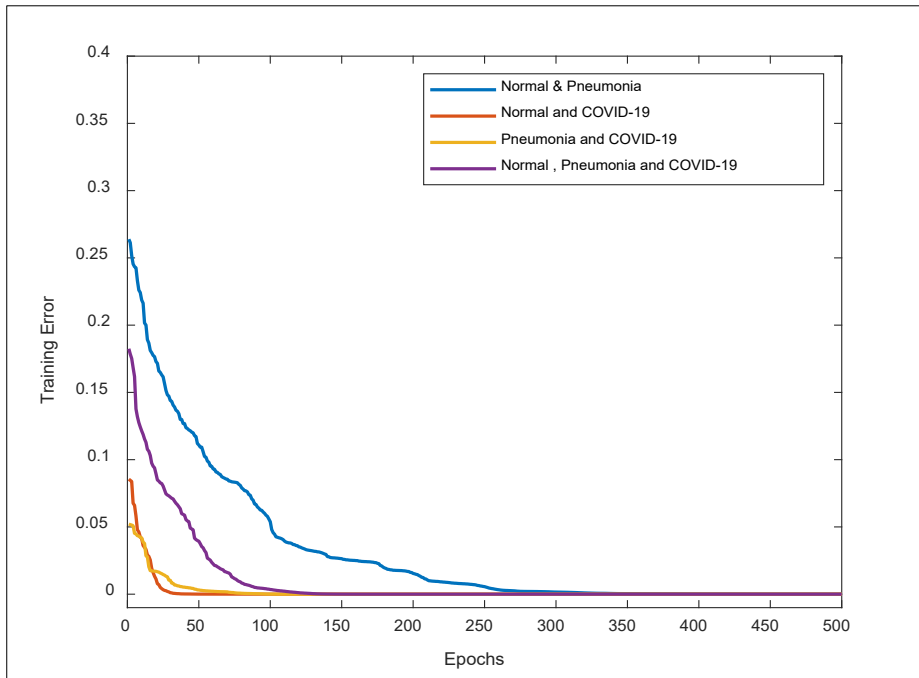


Figure 6. Training performance of the proposed model on X-ray images

Table 3

CT-Scan images result on the test dataset

Sensitivity	Specificity	Precision	F1-Score	Accuracy
81.13%	85.11%	86.00%	83.50%	83.00%

Table 4

X-ray images result on the test dataset

No.	Conditions	Sensitivity	Specificity	Precision	F1-Score	Overall Accuracy
1	Normal & COVID-19	95.6%	92.5%	94.0%	94.95%	94.4%
2	Pneumonia & COVID-19	96.08%	97.37%	98.0%	97.03%	96.6%
3	Normal & Pneumonia	81.13%	85.11%	86.0%	83.5%	83.0%
4	Normal	74.00%	91.01%	82.22%	77.90%	82.0%
	Pneumonia	80.00%	85.39%	75.47%	77.67%	
	COVID-19	94.87%	96.00%	90.24%	92.50%	

Besides, the proposed model has been tested with X-ray image dataset. The dataset has been distributed to four conditions as shown in Table 4. The proposed model achieved 92% to 95.6% for all scores on the first condition. Meanwhile, the model achieved 96 to 98% for all score on the second condition which is the highest performance over other conditions. From the result, it can be noticed that the proposed model can detect accurately the different chest X-ray images between pneumonia and COVID-19 patient. However, the performance of the proposed model dropped when tested with third and fourth conditions of the dataset. This is due to the incapability of the model to detect accurately the different chest X-ray images between normal and pneumonia patient. There is slightly different in the calculation of forth condition datasets as each class has its own scores value except the overall accuracy. From each score on each class, the performance of the proposed model can be observed in each class. From the result of forth condition dataset, the model suffers a difficulty to differentiate the normal and pneumonia patient. Throughout the analysis there is no major overfitting issue occur on the proposed model as there is no big difference in the training and testing performance of the model on both datasets.

The proposed model performance has been compared with the shallow learning model such as an artificial neural network (ANN) and support vector machine (SVM). Both models are the popular shallow models that are always been used in many applications like mechanical engineering, biomedical engineering, and medicine. Hence, both models have been trained and test with chest CT-scan and X-ray images. The diagnosis accuracy is used to compare the performance of shallow leaning model with proposed model method. Bayesian optimisation is used to optimise the hyperparameter of the SVM model. On the CT-scan images as shown in Table 5, the ANN and SVM models, the models achieved 73.3% and 75.5%, respectively. Meanwhile, on the X-ray images as shown in Table 6, the ANN model can achieve more than 80% accuracy on datasets 2 (Pneumonia and COVID-19 dataset). However, the ANN model achieved below 80% for the rest of the datasets. Meanwhile, optimised SVM model achieved more than 80% accuracy on datasets 1 (Normal & COVID-19) and 2 (Pneumonia & COVID-19). However, the optimised SVM model achieved below 80% on datasets 3 (Normal & Pneumonia) and 4 (Normal, Pneumonia & COVID-19). In comparison, the proposed model performance on both images' dataset is more accurate compared to the shallow learning model that shows the capability of deep learning over shallow learning model on image classification analysis.

The proposed model performance is compared with other similar studies as published in public journal that use the convolutional neural network model (Hemdan et al., 2020; Purohit et al., 2020; Wang et al., 2020). Convolutional neural network (CNN) is the common method used in many applications especially for image classification analysis. The comparative study between the proposed model and CNN model is shown in Tables 7 and 8 for CT scan and X-ray images, respectively. On the X-ray images, the comparative study

used normal and COVID-19 conditions. The proposed model performed better compared VGG16 and VGG19 as shown in Table 7 and 8. VGG16 is the CNN model that was used to win the competition of ImageNet in 2014. While VGG19 is the improve version of CNN that has a better performance compared to VGG16 but VGG19. CNN model is known to have more hyperparameter that need to be set compared to the proposed model. This is one of the factors the CNN model is difficult to handle. Meanwhile, another improvement has been conducted by Wang et al. (2020) as the authors tend to use deeper architecture of CNN network on CT scan images. With deeper architecture the number of hyperparameter will increase that cause the network is difficult to handle. However, the result produced by the deeper CNN model is lower compared to the proposed model. According to the result, the proposed model performed significantly better since it uses simple architecture, as mentioned in the preceding section, instead of complicated signal and image processing and deeper learning architecture.

Table 5
CT-Scan images result on the test dataset

Shallow learning	Accuracy
ANN	73.3%
Optimize SVM	75.5%

Table 6
X-ray images result on the test dataset

Datasets	Class distribution	ANN	Optimize SVM
1	Normal & COVID-19	75.0%	81.4%
2	Pneumonia & COVID-19	83.9%	85.1%
3	Normal & Pneumonia	61.4%	75.5%
4	Normal, Pneumonia & COVID-19	62.6%	73.2%

Table 7
Comparative analysis with a similar study on X-ray images

Model	Sensitivity %	Specificity %	Precision %	F1-Score %	Overall Accuracy %
Proposed model	95.6	92.5	94.0	94.95	94.4
Purohit et al. (2020) VGG16	81.52	99.25	99.0	89.0	90.4

Table 7 (Continued)

Model	Sensitivity %	Specificity %	Precision %	F1-Score %	Overall Accuracy %
Hemdan et al. (2020) VGG19	90.0	-	91.5	90.0	90.0

Table 8

Comparative analysis with a similar study on CT scan images

Model	Sensitivity %	Specificity %	Precision %	F1-Score %	Accuracy %
Proposed model	81.13	85.11	86.0	83.5	83.0
Purohit et al. (2020) VGG16	93.62	63.76	72.0	88.0	78.7
Wang et al. (2020) CNN Dens-net	93.0	-	76.0	83.0	82.0

CONCLUSION

This paper has presented an improved SSAE to detect and diagnose COVID-19 on chest CT scan images and chest X-ray images. The proposed model did not require manual feature extraction and it can achieve satisfactory performance on COVID-19 dataset without image enhancement method on the image. This analysis proved that the proposed model can be used on other applications not only on machinery diagnosis. The selection of hyperparameter on deep learning is crucial as it may provide a good diagnosis result. Future research may implement the image enhancement on the dataset with a large size of the dataset to increase the classification accuracy.

ACKNOWLEDGMENT

The authors would like to extend their greatest gratitude to the Institute of Noise and Vibration UTM for funding the current study under the Higher Institution Centre of Excellence (HICoE) Grant Scheme (R.K130000.7843.4J227 and R.J130000.7824.4J234). Additional funding for this research came from the UTM Research University Grant (Q.K130000.2543.11H36) and the Fundamental Research Grant Scheme (R.K130000.7840.4F653) from The Ministry of Higher Education, Malaysia.

REFERENCES

- Apostolopoulos, I. D., & Mpesiana, T. A. (2020). Covid-19: Automatic detection from X-ray images utilizing transfer learning with convolutional neural networks. *Physical and Engineering Sciences in Medicine*, 43(2), 635-640. <https://doi.org/10.1007/s13246-020-00865-4>
- Bustin, S. A., & Nolan, T. (2020). RT-qPCR testing of SARS-CoV-2: A primer. *International Journal of Molecular Sciences*, 21(8), Article 3004. <https://doi.org/10.3390/ijms21083004>
- Cohen, J. P., Morrison, P., Dao, L., Roth, K., Duong, T. Q., & Ghassemi, M. (2020). *GitHub - iee8023/covid-chestxray-dataset: We are building an open database of COVID-19 cases with chest X-ray or CT images*. Retrieved March 22, 2021, from <https://github.com/ieee8023/COVID-chestxray-dataset>
- He, X., Yang, X., Zhang, S., Zhao, J., Zhnag, Y., Xing, E., & Xie, P. (2020). *Sample-efficient deep learning for COVID-19 diagnosis based on CT scans*. Retrieved March 22, 2021, from <https://github.com/UCSD-AI4H/COVID-CT>
- Hemdan, E. E. D., Shouman, M. A., & Karar, M. E. (2020). COVIDX-Net: A framework of deep learning classifiers to diagnose COVID-19 in X-ray images. *ArXiv*, 1-14.
- Huang, C., Wang, Y., Li, X., Ren, L., Zhao, J., Hu, Y., Zhang, L., Fan, G., Xu, J., Gu, X., Cheng, Z., Yu, T., Xia, J., Wei, Y., Wu, W., Xie, X., Yin, W., Li, H., Liu, M., ... & Cao, B. (2020). Clinical features of patients infected with 2019 novel coronavirus in Wuhan, China. *The Lancet*, 395(10223), 497-506. [https://doi.org/10.1016/S0140-6736\(20\)30183-5](https://doi.org/10.1016/S0140-6736(20)30183-5)
- Luo, L., Xiong, Y., Liu, Y., & Sun, X. (2019). Adaptive gradient methods with dynamic bound of learning rate. *ArXiv:1902.09843, 2018*, 1-19.
- Ozturk, T., Talo, M., Yildirim, E. A., Baloglu, U. B., Yildirim, O., & Acharya, U. R. (2020). Automated detection of COVID-19 cases using deep neural networks with X-ray images. *Computers in Biology and Medicine*, 121, Article 103792. <https://doi.org/10.1016/j.compbiomed.2020.103792>
- Purohit, K., Kesarwani, A., Kisku, D. R., & Dalui, M. (2020). COVID-19 detection on chest X-Ray and CT scan images using multi-image augmented deep learning model. *BioRxiv*, 15-22. <https://doi.org/10.1101/2020.07.15.205567>
- Riedmiller, M., & Braun, H. (1993). A direct adaptive method for faster backpropagation learning: The RPROP algorithm. In *IEEE international conference on neural networks* (pp. 586-591). IEEE Conference Publication. <https://doi.org/10.1109/ICNN.1993.298623>
- Salehi, S., Abedi, A., Balakrishnan, S., & Gholamrezanezhad, A. (2020). Coronavirus disease 2019 (COVID-19): A systematic review of imaging findings in 919 patients. *American Journal of Roentgenology*, 215(1), 87-93. <https://doi.org/10.2214/AJR.20.23034>
- Saufi, S. R., Ahmad, Z. A., Leong, M. S., & Lim, M. H. (2019). Challenges and opportunities of deep learning models for machinery fault detection and diagnosis: A review. *IEEE Access*, 7(1), 122644-122662. <https://doi.org/10.1109/ACCESS.2019.2938227>
- Srivastava, N., Hinton, G., Krizhevsky, A., Sutskever, I., & Salakhutdinov, R. (2014). Dropout: A simple way to prevent neural networks from overfitting. *Journal of Machine Learning Research*, 15, 1929-1958. <https://doi.org/10.1214/12-AOS1000>

- Tharwat, A. (2018). Classification assessment methods. *Applied Computing and Informatics*, 17(1), 168-192. <https://doi.org/10.1016/j.aci.2018.08.003>
- Verstraete, D., Ferrada, A., Droguett, E. L., Meruane, V., & Modarres, M. (2017). Deep learning enabled fault diagnosis using time-frequency image analysis of rolling element bearings. *Hindawi Shock and Vibration*, 2017, 1-29. <https://doi.org/10.1155/2017/5067651>
- Wahab, M. N. A., Nefti-Meziani, S., & Atyabi, A. (2015). A comprehensive review of swarm optimization algorithms. *PLoS ONE*, 10(5), 1-36. <https://doi.org/10.1371/journal.pone.0122827>
- Wang, S., Kang, B., Ma, J., Zeng, X., Xiao, M., Guo, J., Cai, M., Yang, J., Li, Y., Meng, X., & Xu, B. (2020). A deep learning algorithm using CT images to screen for Corona Virus Disease (COVID-19). *MedRxiv*, 1-23. <https://doi.org/https://doi.org/10.1101/2020.02.14.20023028>
- Wang, Y., Liu, M., Bao, Z., & Zhang, S. (2018). Stacked sparse autoencoder with PCA and SVM for data-based line trip fault diagnosis in power systems. *Neural Computing and Applications*, 5, 1-13. <https://doi.org/10.1007/s00521-018-3490-5>
- Ying, S., Zheng, S., Li, L., Zhang, X., Zhang, X., Huang, Z., Chen, J., Zhao, H., Wang, R., Chong, Y., Shen, J., Zha, Y., & Yang, Y. (2020). Deep learning enables accurate diagnosis of novel Coronavirus (COVID-19) with CT images. *MedRxiv*, 1-10. <https://doi.org/10.1101/2020.02.23.20026930>
- Yang, W., Sirajuddin, A., Zhang, X., Liu, G., Teng, Z., Zhao, S., & Lu, M. (2020). The role of imaging in 2019 novel coronavirus pneumonia (COVID-19). *European Radiology*, 30, 4874-4882. <https://doi.org/10.1007/s00330-020-06827-4>
- Yang, X., He, X., Zhao, J., Zhang, Y., Zhang, S., & Xie, P. (2020). COVID-CT-dataset: A CT scan dataset about COVID-19. *ArXiv Preprint ArXiv:2003.13865*, 1-14.
- Zheng, C., Deng, X., Fu, Q., Zhou, Q., Feng, J., Ma, H., Liu, W., & Wang, X. (2020). Deep learning-based detection for COVID-19 from chest CT using weak label. *MedRxiv*, 1-13. <https://doi.org/10.1101/2020.03.12.20027185>
- Zu, Z. Y., Jiang, M. D., Xu, P. P., Chen, W., Ni, Q. Q., Lu, G. M., & Zhang, L. J. (2020). Coronavirus disease 2019 (COVID-19): A perspective from China. *Radiology*, 296(2), E15-E25. <https://doi.org/10.1148/radiol.202000490>

